Hypernucleus formation and strangeness production in proton-nucleus reactions *

W. Cassing[2], Z. Rudy[1], L. Jarczyk[1], B. Kamys[1],
P. Kulessa[1], O. W. B. Schult[3], A. Sibirtsev[2], A. Strzałkowski[1]

[1] Institute of Physics, Jagellonian University,
Reymonta 4, PL-30059 Cracow, Poland
[2] Institut für Theoretische Physik,
Heinrich-Buff-Ring 16, D-35392 Giessen, Germany
[3] Experimentelle Kernphysik II, Forschungszentrum Jülich,
D-52425 Jülich, Germany

Abstract

We study the production of Λ hyperons in $p + A$ reactions on the basis of a BUU transport approach from 1.1 to 1.9 GeV and evaluate the properties of the hypernuclei produced in particular with respect to their momentum distribution in the laboratory frame. Due to elastic ΛN scattering large cross sections for the production of heavy hypernuclei in the order of 100 - 400 μb are predicted for p + U at 1.5 - 1.9 GeV laboratory energy. Whereas the K^+Y production channels are expected to be only slightly modified in the nuclear medium, the antikaon production should be enhanced substantially due to large attractive K^- selfenergies in dense matter. We predict an enhancement of the inclusive K^- yield in p + ^{208}Pb collisions of a factor of ≈ 10 at 2 GeV laboratory energy.

1 Introduction

The investigation of strangeness in hadrons and nuclei has become an exciting and challenging field of research in the last years [1]. Here, the open questions reach from the spectroscopy of hypernuclei to the formation of strange hadronic matter in neutron stars or ultrarelativistic nucleus-nucleus collisions. Whereas earlier studies were devoted to the production aspects of hyperons and strange mesons, nowadays, the interest is moving towards the properties of strange particles in a nuclear environment.

Λ-hypernuclei are especially well suited for in-medium strangeness investigations since the Λ-hyperon has a long lifetime as compared to the nuclear scale. The 'free'

*Supported by Forschungszentrum Jülich and the Polish Committee for Scientific Research

Λ-hyperon decay is purely mesonic ($\Lambda \to N\pi$) whereas in the nuclear medium also non-mesonic decay channels ($\Lambda N \to NN$) are possible. The competition between these decay modes is expected to provide information about the hypernuclear structure (e.g. the Λ and pion selfenergies in the nuclear medium) [2]. Since the lifetime of the hypernucleus depends on the corresponding widths of these decays , i.e. $\tau = \hbar$ / [$\Gamma_{mes} + \Gamma_{nonmes}$], it is of considerable interest to measure the lifetime of hypernuclei as a function of their mass, particularly for heavy systems, where Γ_{mes} is strongly suppressed due to Pauli blocking [3] such that Γ_{nonmes} is directly related to τ^{-1}.

This particular question has been investigated with antiproton beams on ^{209}Bi and ^{238}U targets in [4]. However, the lifetimes of $^{209}_{\Lambda}$Bi and $^{238}_{\Lambda}$U from this experiment are quite different contrary to simple phase-space expectations. Alternatively, one might investigate the production of heavy hypernuclei by means of proton + nucleus reactions. In fact, the recent studies on the (p , K^+) reaction confirm a quite substantial production of associated Λ-hyperons [5, 6] leading to production cross sections for Λ-hypernuclei in the order of a few 100 μb for p + Pb at 1.5 - 1.9 GeV [3, 7].

Apart from the lifetime of the Λ hyperon in the medium also the kaon and antikaon properties should change due to interactions with the nuclear environment [8, 9, 10]. Whereas the K^+ potential is expected to be slightly repulsive in the medium, the K^- meson should see a sizeable attractive potential in dense matter such that their production should be enhanced at finite baryon density. In case of heavy-ion collisions a first exploratory study has been performed by Li, Ko and Fang [11] with the result that large attractive K^- potentials are needed to explain the experimental spectra from [12] for Ni + Ni at 1.85 AGeV. A more systematic transport analysis - including all possible production channels - on this question has been performed in Refs. [13, 14] in comparison to the recent data from the KaoS Collaboration [15]. In fact, the experimental data indicate an attractive K^- potential of about -100 MeV at normal nuclear matter density ($\rho_0 \approx 0.16$ fm^{-3}) whereas the K^+ potential at density ρ_0 is in the range between 0 and +30 MeV [13, 14]. Such effects should also be seen and probed experimentally in p + A reactions at subthreshold energies.

In continuation of our earlier work [3, 7] we here present a transport (BUU) analysis of proton + nucleus collision events, including the production channels $pN \to NYK^+$ and $\pi N \to YK^+$ (Y = Λ, Σ), while nonperturbatively taking into account the rescattering of the hyperons with nucleons and the hyperon propagation in the nuclear mean field.

2 Ingredients of the transport approach

In this contribution we perform our analysis along the line of the HSD[1] approach [17] which is based on a coupled set of covariant transport equations for the phase-space distributions $f_h(x,p)$ of hadron h, i.e.

$$\left\{\left(\Pi_\mu - \Pi_\nu \partial^p_\mu U^\nu_h - M^*_h \partial^p_\mu U^S_h\right)\partial^\mu_x + \left(\Pi_\nu \partial^x_\mu U^\nu_h + M^*_h \partial^x_\mu U^S_h\right)\partial^\mu_p\right\} f_h(x,p)$$

[1]Hadron String Dynamics

$$= \sum_{h_2 h_3 h_4 \ldots} \int d2d3d4 \ldots [G^\dagger G]_{12\to 34\ldots} \delta^4(\Pi + \Pi_2 - \Pi_3 - \Pi_4 \ldots)$$
$$\times \Big\{ f_{h_3}(x,p_3) f_{h_4}(x,p_4) \bar{f}_h(x,p) \bar{f}_{h_2}(x,p_2)$$
$$- f_h(x,p) f_{h_2}(x,p_2) \bar{f}_{h_3}(x,p_3) \bar{f}_{h_4}(x,p_4) \Big\} \ldots \quad . \tag{1}$$

In Eq. (1) $U_h^S(x,p)$ and $U_h^\mu(x,p)$ denote the real part of the scalar and vector hadron selfenergies, respectively, while $[G^+G]_{12\to 34\ldots}\delta^4(\Pi + \Pi_2 - \Pi_3 - \Pi_4 \ldots)$ is the 'transition rate' for the process $1+2 \to 3+4+\ldots$ which is taken to be on-shell in the semiclassical limit adopted. The hadron quasi-particle properties in (1) are defined via the mass-shell constraint

$$\delta(\Pi_\mu \Pi^\mu - M_h^{*2}) \quad , \tag{2}$$

with effective masses and momenta (in local Thomas-Fermi approximation) given by

$$\begin{aligned} M_h^*(x,p) &= M_h + U_h^S(x,p) \\ \Pi^\mu(x,p) &= p^\mu - U_h^\mu(x,p) \quad , \end{aligned} \tag{3}$$

while the phase-space factors

$$\bar{f}_h(x,p) = 1 \pm f_h(x,p) \tag{4}$$

are responsible for fermion Pauli-blocking or Bose enhancement, respectively, depending on the type of hadron in the final/initial channel. The dots in Eq. (1) stand for further contributions to the collision term with more than two hadrons in the final/initial channels. The transport approach (1) is fully specified by $U_h^S(x,p)$ and $U_h^\mu(x,p)$ ($\mu = 0,1,2,3$), which determine the mean-field propagation of the hadrons, and by the transition rates $G^\dagger G\, \delta^4(\ldots)$ in the collision term, that describes the scattering and hadron production/absorption rates.

The scalar and vector mean fields U_h^S and U_h^μ for nucleons are taken from Ref. [17]; the hyperon mean fields are assumed to 2/3 of the nucleon potentials. In the present approach, apart from nucleons, $\Delta, N(1440)$, $N(1535)$, Λ, Σ with their isospin degrees of freedom, we propagate explicitly pions, K^+, K^-, and η's and assume that the pions as Goldstone bosons do not change their properties in the medium; we also discard selfenergies for the η-mesons which have a minor effect on the K^+, K^- dynamics. The kaon and antikaon potentials, however, have to be specified more explicitly.

2.1 K^+, K^- selfenergies

There are a couple of models for the kaon and antikaon selfenergies [8, 9, 10], which differ in the actual magnitude of the selfenergies, however, agree on the relative signs for kaons and antikaons. Thus in line with the kaon-nucleon scattering amplitude the K^+ potential should be slightly repulsive at finite baryon density whereas the antikaon should see an attractive potential in the nuclear medium. Without going into a detailed discussion of the various models we adopt the more practical point of view, that the

actual K^+ and K^- selfenergies are unknown and as a guide for our analysis use a linear extrapolation of the form,

$$m_K^*(\rho_B) = m_K^0 \left(1 + \alpha \frac{\rho_B}{\rho_0}\right), \tag{5}$$

with $\alpha \approx$ -0.2 for antikaons and $\alpha \approx 0.06$ for kaons (or $\alpha = 0$ for the bare kaon). Our choice ($\alpha \approx$ -0.2) leads to a fairly reasonable reproduction of the antikaon mass from Ref. [9] (thin solid line in Fig. 1) and the recent results from Waas, Kaiser and Weise [10] (thick solid line in Fig. 1). We note that the dropping of the antikaon mass is associated with a corresponding scalar energy density in the baryon/meson Lagrangian, such that the total energy-momentum is conserved during the heavy-ion collision (cf. [17]).

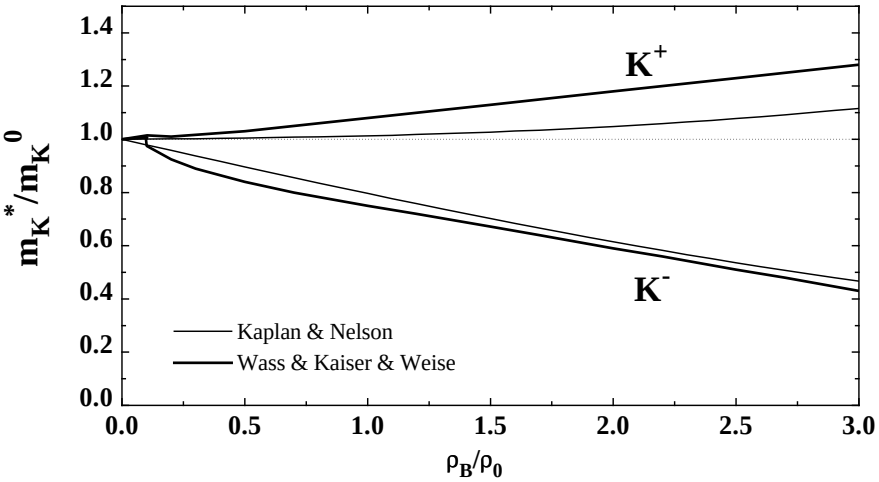

Fig. 1: The K^+, K^- mass as a function of the baryon density in units of $\rho_0 \approx 0.16 fm^{-3}$ according to Kaplan and Nelson [9] (thin solid lines) and Waas, Kaiser and Weise [10] (thick solid lines).

2.2 Perturbative treatment of strangeness production

The calculation of 'subthreshold' particle production is described in detail in Ref. [16] and has to be treated perturbatively in the energy regime of interest here due to the small cross sections involved. Since we work within the parallel ensemble algorithm, each parallel run of the transport calculation can be considered approximately as an individual reaction event, where binary reactions in the entrance channel at given invariant energy $\sqrt{s}$ lead to final states with 2 (e.g. K^+Y in πB channels), 3 (e.g. for K^+YN channels in BB collisions) or 4 particles (e.g. $K\bar{K}NN$ in BB collisions) with a relative weight W_i for each event i which is defined by the ratio of the production cross section to the total hadron-hadron cross section[2]. We thus dynamically gate on all events where a K^+Y or K^+K^- pair is produced initially. Each strange hadron then is represented by a testparticle with weight W_i and propagated according to the Hamilton equations

[2]The actual final states are chosen by Monte Carlo according to the 2, 3, or 4-body phase space.

of motion. Elastic and inelastic reactions with pions, η's or nonstrange baryons are computed in the standard way [16] and the final cross section is obtained by multiplying each testparticle with its weight W_i. In this way one achieves a realistic simulation of the strangeness production, propagation and reabsorption during the heavy-ion collision.

For further details of the model and the explicit parametrizations of the various reaction cross sections we refer the reader to Refs. [3, 16, 13, 14], respectively.

3 Recoil momentum distributions

Since in the transport calculations the four-momenta of all hadrons are propagated in time we are capable to extract for events, leading to hypernucleus formation, the average properties of the residual hypernucleus. For this purpose we compute as a function of time those particles (essentially nucleons) that have left the residual heavy fragment at position $\mathbf{R}$, i.e.

$$|\mathbf{r}_i - \mathbf{R}| \geq R_A + 2fm, \tag{6}$$

where $R_A = 1.2fm\ A_t^{1/3}$ denotes the radius of the target with mass number A_t. Now let the number of particles emitted be $N_p(t)$. For each parallel ensemble we can then evaluate the fragment's average mass number, its excitation energy, three-momentum and angular momentum by exploring the conservation of total energy, mass number, momentum and angular momentum:

$$\begin{aligned}
< E^* > (t) &= E_{tot} - \sum_{j=1}^{N_p(t)} \sqrt{p_j^2 + M_j^2} - M_{res} - E_{coul} - M_\Lambda + M_N - E_K, \\
< A_F > (t) &= A_t + 1 - N_p(t), \\
< \mathbf{p} > (t) &= \mathbf{P}_{tot} - \sum_{j=1}^{N_p(t)} \mathbf{p}_j(t), \\
< \mathbf{L} > (t) &= \mathbf{L}_{tot} - \sum_{j=1}^{N_p(t)} \mathbf{r}_j(t) \times \mathbf{p}_j(t).
\end{aligned} \tag{7}$$

In eq. (7) M_{res} denotes the mass of the 'residual nucleus', E_{coul} stands for the Coulomb energy between the emitted particles and the 'residual nucleus', while E_K represents the total energy of the K^+-meson.

All quantities in (7) depend explicitly on time t due to the continuous evaporation of particles from the final compound system. Since we will follow the further decay chains by statistical model codes, the actual transition time for the connection of the BUU and the statistical model calculation is of no significance as long as the system has left the nonequilibrium phase of the reaction and achieved statistical equilibrium. We have checked that it is sufficient to trace the history of each ensemble of events within BUU up to 150 fm/c [7].

As an example for the momentum distribution of hypernuclei we show in Fig. 2 the computed distributions in beam direction (dN/p_z) and perpendicular to the beam (dN/dp_x) for p + ^{238}U at T_{lab} = 1.5 GeV from the BUU calculation (dashed lines) as

well as after particle evaporation (solid lines) computed via PACE2 [18, 7]. We note that the particle evaporation only broadens the momentum distribution somewhat, but does not change the average momentum per particle in the beam direction.

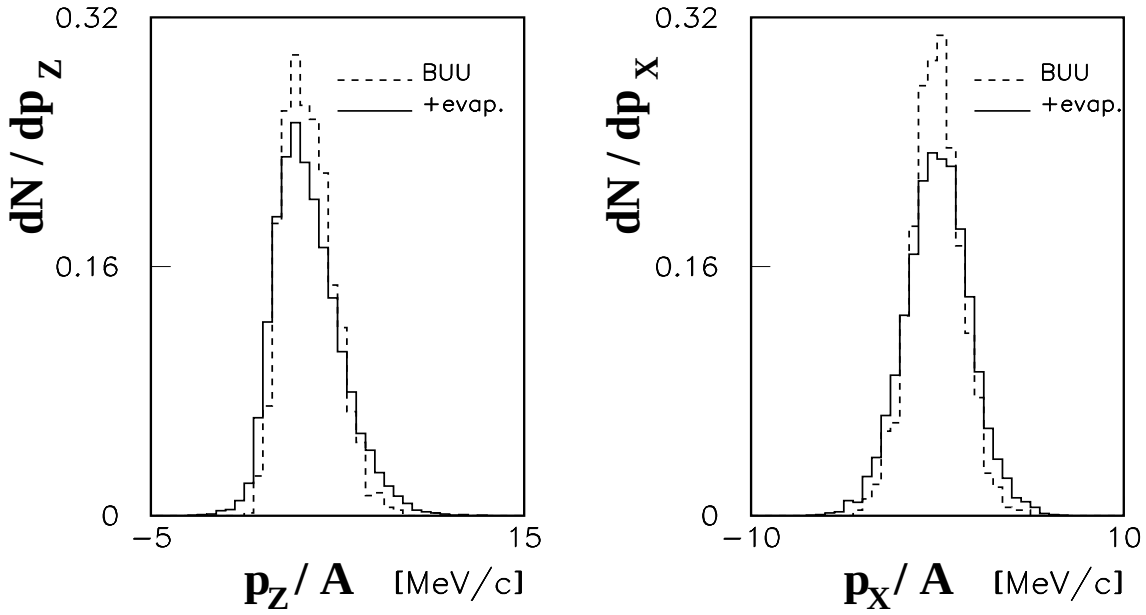

Fig. 2: Longitudinal momentum (p_z/A) and transverse momentum (p_x/A) distribution of Λ-hypernuclei at $T_{lab} = 1.5$ GeV for p + ^{238}U with evaporation (solid histograms) and without evaporation (dashed histograms).

Since the computed momentum distributions enter as an important ingredient in the experimental analysis [19, 20] based on the recoil shadow method, we have to investigate the accuracy of the transport calculations with respect to the momentum transfer in proton-nucleus reactions. In this respect we show in Fig. 3 the longitudinal momentum distribution of the residual nuclei from the BUU calculation (solid histograms) - without gating on hypernuclei - for p + ^{238}U at $T_{lab} = 475$ MeV, 1.0 GeV, 1.5 GeV, and 2.9 GeV in comparison to the data of Fraenkel et al. [21] (full squares) and Kotov et al. [22]. The good agreement with the data in this wide kinematical regime demonstrates the relative accuracy of the transport approach which should be of the same quality when gating on events with hypernucleus formation (cf. Fig. 2).

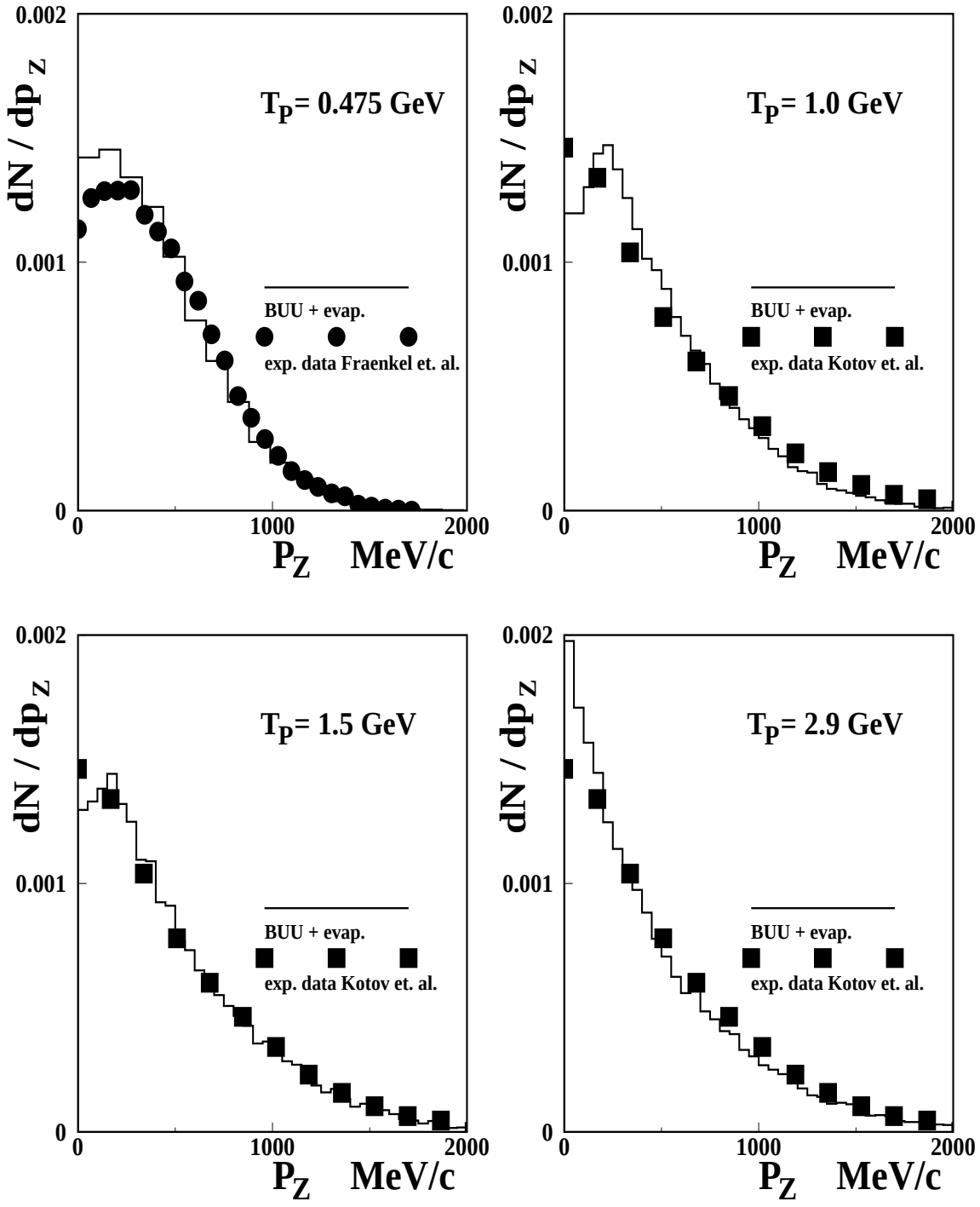

Fig. 3: Comparison of the longitudinal momentum distribution for p + ^{238}U at T_{lab} = 475 MeV (lhs. top), 1.0 GeV, 1.5 GeV, and 2.9 GeV from the BUU calculation (solid histograms) with the data from Fraenkel et al. [21] and Kotov et al. [22] (full squares).

4 K^+ and K^- production in p + A collisions

The inclusive production of kaons and hypernuclei in p + A collisions has been studied at subthreshold energies to a large extend in Ref. [5, 6, 3] and does not have to be reviewed here. The novel aspects are those related to antikaons and their selfenergy or potential inside heavy nuclei. Since antikaon production has a threshold of about 2.5 GeV in free nucleon-nucleon collisions, we have to address the question of kaon production at $T_{lab} \approx$ 2 - 3 GeV, too.

In this respect we first compare our calculations (solid histograms) with the experimental K^+ spectra for p + Pb at 2.1 GeV from Schnetzer et al. [23] in Fig. 4 without including any medium modification of the kaons (in line with the hypothesis of Kaplan and Nelson [9] (cf. Fig. 1)). Indeed, the experimental spectra are described quite accurately as in case of nucleus-nucleus collisions at SIS energies [14] without any selfenergies such that a measurement of K^-/K^+ ratios at the same bombarding energy becomes interesting due to its sensitivity to the antikaon potentials.

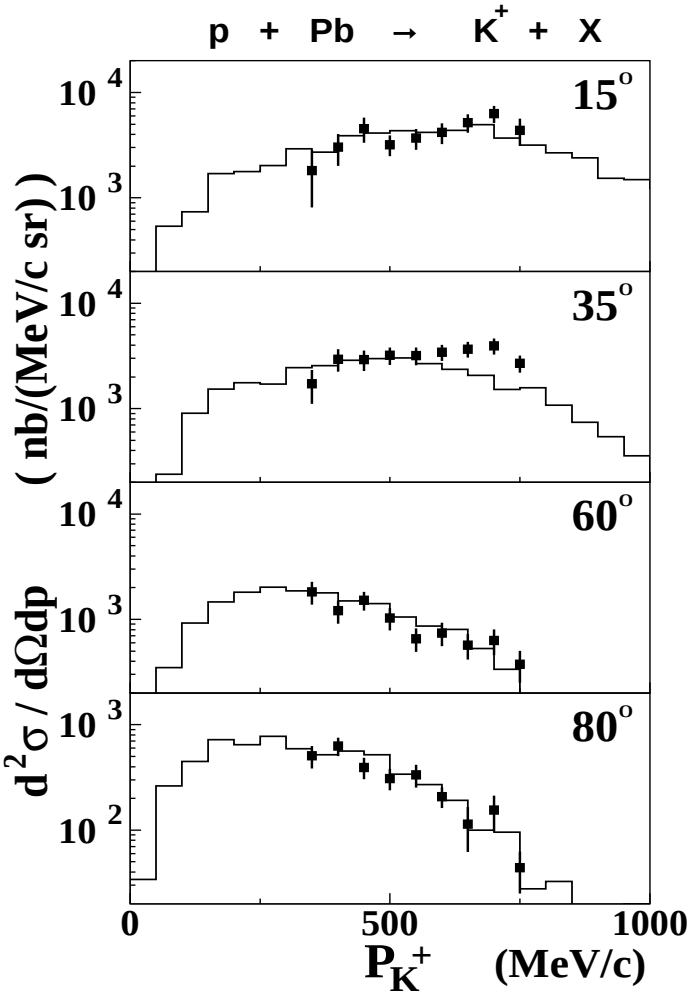

Fig. 4: The calculated K^+ spectra for p + Pb collisions (solid lines) at 2.1 GeV in comparison to the data from Schnetzer et al. [23] at various angles θ_{lab} in the laboratory.

Employing the various production channels for antikaons ($pN \to NNK\bar{K}, \pi N \to NK\bar{K}, \pi Y \to N\bar{K}, YN \to NN\bar{K}$) as well as antikaon absorption ($\bar{K}N \to \pi Y$) from Ref. [13] we have performed detailed calculations on the K^+ and K^- spectra in p + ^{208}Pb collisions from 2 - 3 GeV bombarding energy. The first predictions for the total K^-/K^+ ratio are presented in Fig. 5 (integrated over all momenta) as a function of T_{lab} for a bare antikaon mass (open squares) and an in-medium antikaon mass (full dots) according to Eq. (5) with α = -0.2 which corresponds to an attractive antikaon potential of about -100 MeV at ρ_0. We find the K^-/K^+ ratio to increase from 2×10^{-4} to 7×10^{-3} in this energy regime for the bare antikaon case; however, when including the attractive K^- potential the ratio is enhanced by about a factor of 10 at T_{lab} = 2 GeV and by a factor of $\approx$ 2 at T_{lab} = 3 GeV.

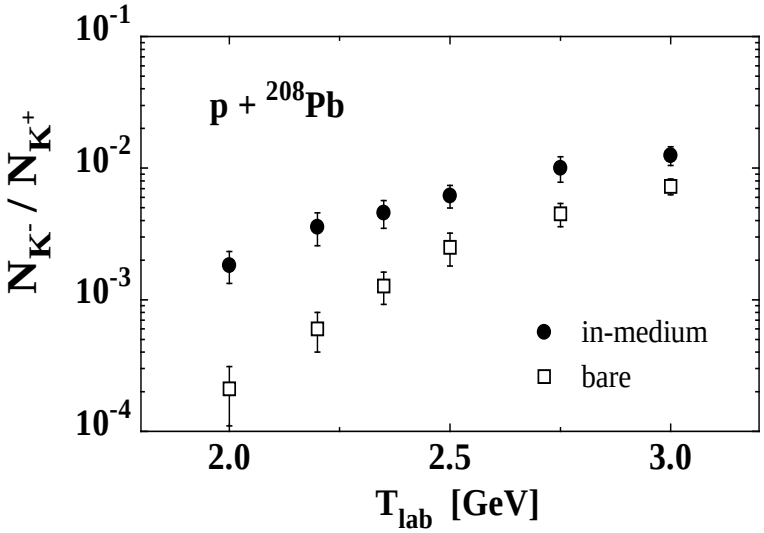

Fig. 5: The calculated K^-/K^+ ratio for p + ^{208}Pb reactions from 2 to 3 GeV; with an attractive antikaon potential (full dots); without antikaon potential (open squares).

5 Summary and conclusion

In this study we have presented a BUU transport analysis of K^+Y and K^+K^- production in proton + nucleus collisions at COSY energies employing the elementary production processes from our earlier work [6, 13]. Due to a large fraction of Λ hyperons from the secondary process $\pi N \to K^+\Lambda$, which leads to hyperons with moderate momenta in the laboratory system, the p+nucleus reaction efficiently produces heavy hypernuclei and cross sections of about a few 100 μb are expected for p + ^{208}Pb at 1.5 - 1.9 GeV [3], which is in line with present experimental data so far [19, 20].

We have, furthermore, shown that the transport approach also reliably describes the momentum transfer to the target nucleus in a wide kinematical regime from 475 MeV to 2.9 GeV for heavy nuclei such that the computed momentum distributions for hypernuclei, that are needed for the experimental analysis [19, 20] based on the recoil shadow method, are expected to have the same accuracy.

In addition, we have explored the possibility to measure the K^- potential in finite nuclei via their production cross section relative to K^+ mesons. In fact, p + ^{208}Pb reactions at 2.0 GeV indicate an increase of the K^- cross section about a factor of 10 when including a K^- potential of about -100 MeV at ρ_0 (cf. Fig. 1) in line with the chiral Lagrangians of [9, 10] and the analysis in Ref. [13]. This enhancement should be clearly seen in the next generation of experiments.

References

[1] Proceedings of the International Symposium on Hypernuclear and Strange Particle Physics (20th INS International Symposium), Nucl. Phys. **A547** (1992)

[2] T. Motoba, Nucl. Phys. **A527** (1991) 485c; Nucl. Phys. **A547** (1992) 115c

[3] Z. Rudy et al., Z. Phys. **A351** (1995) 217

[4] T. A. Armstrong et al., Phys. Rev. **C47** (1993) 1957

[5] W. Cassing et al., Phys. Lett. **B238** (1990) 25

[6] W. Cassing et al., Z. Phys. **A349** (1994) 77

[7] Z. Rudy et al., Z. Phys. **A354** (1996) 445

[8] G. E. Brown, C. M. Ko, Z. G. Wu, and L. H. Xia, Phys. Rev. **C 43** (1991) 1881.

[9] D. B. Kaplan and A. E. Nelson, Phys. Lett. **B 175** (1986) 57.

[10] T. Waas, N. Kaiser, and W. Weise, Phys. Lett. **B 379** (1996) 34.

[11] G. Q. Li, C. M. Ko, and X. S. Fang, Phys. Lett. **B329** (1994) 149

[12] A. Schröter et al., Z. Phys. **A350** (1994) 101.

[13] W. Cassing et al., Nucl. Phys. **A614** (1997) 415

[14] E. L. Bratkovskaya, W. Cassing and U. Mosel, Nucl. Phys. **A622** (1997) 593.

[15] P. Senger et al., Acta Physica Polonica **B 27** (1996) 2993

[16] W. Cassing et al., Phys. Rep. **180** (1990) 363

[17] W. Ehehalt and W. Cassing, Nucl. Phys. **A 602** (1996) 449.

[18] A. Gavron, in 'Computational Nuclear Physics', Vol. 2 'Nuclear Reactions', ed. by Langanke, K., Maruhn, J. A. and Koonin, S. E., Springer Verlag 1993, p. 108

[19] H. Ohm et al., Phys. Rev. **C55** (1997) 3062.

[20] L. Jarczyk et al., these proceedings

[21] Z. Fraenkel et al., Phys. Rev. **C41** (1990) 1050

[22] A. A. Kotov et al., Sov. J. Nucl. Phys. **17** (1974) 498; **19** (1974) 385

[23] S. Schnetzer et al., Phys. Rev. **C40** (1989) 640